How to cite: *Angew. Chem. Int. Ed.* **2025**, *64*, e202505083
doi.org/10.1002/anie.202505083

Macrocycles **Hot Paper**

Catching Fullerenes: Synthesis of Molecular Nanogloves

*Saber Mirzaei, Hormoz Khosravi, Xiangquan Hu, M. Saeed Mirzaei, Victor M. Espinoza Castro, Xu Wang, Nicholas A. Figueroa, Tieyan Chang, Ying-Pin Chen, Gabriella Prieto Ríos, Natalia Isabel Gonzalez-Pech, Yu-Sheng Chen, and Raúl Hernández Sánchez**

Abstract: Herein, we report the synthesis of a new series of rigid, all *meta*-phenylene, conjugated deep-cavity molecules, displaying high binding affinity towards buckyballs. A facile synthetic approach with an overall combined yield of approximately 53% in the last two steps has been developed using a templating strategy that combines the general structure of resorcin[4]arene and [12]cyclo-*meta*-phenylene. These two moieties are covalently linked via four acetal bonds, resulting in a glove-like architecture. ^{1}H NMR titration experiments reveal fullerene binding affinities (K_a) exceeding $\geq 10^6$ M^{-1}. The size complementarity between fullerenes and these scaffolds maximizes CH$\cdots\pi$ and $\pi\cdots\pi$ interactions, and their host:guest adduct resembles a ball in a glove, hence their name as nanogloves. Fullerene recognition is tested by suspending carbon soot in a solution of nanoglove in 1,1,2,2-tetrachloroethane, where more than a dozen fullerenes are observed, ranging from C_{60} to C_{96}.

Introduction

Macrocycles with well-defined shapes and cavities have been targeted as building blocks in nanoscience,[1] with applications spanning organic nanodevices,[2] host-guest chemistry,[3,4] sensors,[5,6] optoelectronic materials,[7] biomedical applications,[8,9] and petrochemical separations.[10] Cyclophenylenes fall under the definition of conjugated macrocycles with an almost century-long history. Cyclo-*ortho*-phenylenes (COPs) were first reported in the 1940s,[11–16] and were later followed by cyclo-*meta*-phenylenes (CMPs) in the 1960s.[17–23] The radial nature of cyclo-*para*-phenylenes (CPPs) made them a challenging synthetic target for decades up until their first report in 2008.[24,25] Moreover, the synthesis of cyclophenylenes with mixed connectivity, for example, integrating *meta*- and *para*-phenylenes within the same macrocycle, has been reported to create compounds with unique fluorescent properties and applications in cellular imaging.[26,27] The evolution of cyclophenylenes has paved the way to realize architectures that were previously only hypothetical, such as carbon nanobelts,[28–30] Möbius topologies,[31–33] and a large number of contorted aromatic compounds.[34–36] Despite synthetic progress on cyclophenylenes, access to large [*n*]CMPs (n > 10) remains a challenge,[23] likely due to unfavourable entropic contribution during the ring closure step.[37] Therefore, template-based syntheses of cyclophenylenes provide a unique approach to solve current challenges in the field.

For decades, macrocyclic arenes, such as calix[*n*]arenes, resorcin[*n*]arenes, calix[*n*]pyrroles, pillar[*n*]arenes, pyrogallol[*n*]arenes, and several others, have been active players in establishing fundamental principles in supramolecular chemistry.[38] Lately, some of these families have been used in the formation of conjugated macrocycles as reported by Itami,[39–41] Chen,[42,43] Wang,[44] and Lucas.[45] Interested in merging ideas of conjugated and nonconjugated macrocycles, as previously demonstrated with calix[*n*]arenes,[46–49] our group and others have been working on an approach using resorcin[*n*]arenes to template and direct the growth of conjugated architectures.[50–52] Advancing our previous work, we set out to incorporate [*n*]CMPs and resorcinarenes into a single scaffold. As a result, we obtained a class of compounds with a remarkable binding affinity for fullerenes, where the host-guest adduct resembles a ball in a baseball glove, thus we decided to call these architectures nanogloves

[*] S. Mirzaei, H. Khosravi, X. Hu, M. S. Mirzaei, V. M. E. Castro, R. Hernández Sánchez
Department of Chemistry, Rice University, 6100 Main St., Houston, Texas 77005, USA
E-mail: raulhs@rice.edu

S. Mirzaei, G. P. Ríos, R. Hernández Sánchez
Department of Chemistry, University of Pittsburgh, 219 Parkman Ave., Pittsburgh, Pennsylvania 15260, USA

X. Wang
Shared Equipment Authority, Rice University, 6100 Main St., Houston, Texas 77005, USA

N. A. Figueroa, N. I. Gonzalez-Pech
Department of Chemistry, Hope College, Holland, Michigan 49423, USA

T. Chang, Y.-P. Chen, Y.-S. Chen
ChemMatCARS, The University of Chicago, Lemont, Illinois 60439, USA

R. Hernández Sánchez
Rice Advanced Materials Institute, Rice University, Houston, Texas, USA

Additional supporting information can be found online in the Supporting Information section

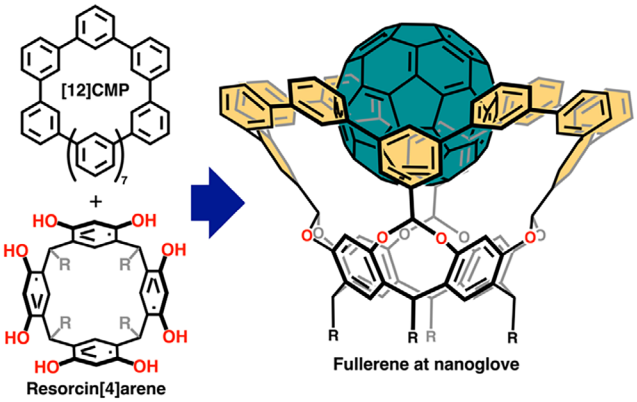

Figure 1. Nanoglove structure. The 1:1 H:G adduct of nanglove:C_{60} is shown on the right-hand side. The top section is a [12]CMP (shaded in yellow) while the bottom part is a resorcin[4]arene.

(Figure 1). Herein, we report the synthetic methodology to obtain nanogloves, their characterization, and their binding affinity and selectivity towards fullerenes.

Results and Discussion

Synthesis

Nanogloves are obtained in high yields from *n*-pentyl[53] or *n*-undecyl[54] resorcin[4]arene, $\mathbf{4_5}$ and $\mathbf{4_{11}}$, respectively (Figure 2a). These resorcinarenes were derivatized with 3,5-dibromobenzal bromide (**S1**) in dimethylacetamide (DMA) under basic conditions using DBU (1,8-diazabicyclo[5.4.0]undec-7-ene),[55] to obtain $\mathbf{3_5}$ and $\mathbf{3_{11}}$ in 31 and 32% yield, respectively. Note that the gram-scale synthesis of $\mathbf{3_{11}}$ has been previously reported by Gibb and coworkers in 2007.[56] Suzuki–Miyaura cross coupling of $\mathbf{3_R}$ with 3-chlorophenyl boronic acid, or a substituted version at the fifth position, results in $\mathbf{2X_R}$ (X = **a**, E = H; X = **b**, E = Me; X = **c**, E = OMe). The isolated yield of $\mathbf{2a_5}$ and $\mathbf{2a_{11}}$ is ~90%, which is remarkably high considering eight C─C bonds are formed in this step. The macrocyclization step towards $\mathbf{1X_R}$ was carried out in a nitrogen-filled glovebox employing a Ni-mediated Yamamoto coupling using a 1:1 solvent mixture of toluene:DMF, 2,2′-bipyridine, and $Ni(cod)_2$, as the source of Ni(0), at 80 °C. Aside from $\mathbf{1a_5}$, which was isolated in 32% yield, all three other $\mathbf{1X_{11}}$ were obtained at around 60% isolated yield. Note that $\mathbf{1a_5}$ displays poor solubility in common organic solvents like $CHCl_3$ and CH_2Cl_2; hence, we focused on $\mathbf{1X_{11}}$ for subsequent studies. The structures of $\mathbf{1X_R}$ are expected to be rigid, thus its solubility profile is essentially dictated by its R group.

MALDI MS characterization of all three $\mathbf{1X_{11}}$ compounds perfectly matched their simulated isotopic patterns (Figure 2b). The ^{1}H NMR of $\mathbf{1X_{11}}$ reveals their ideal C_{4v} symmetry in solution (Supporting Information). It is clear from Figure 2c how resonances "b", "c", and "d" shift upfield from $\mathbf{1a_{11}}$, $\mathbf{1b_{11}}$, to $\mathbf{1c_{11}}$ as the substituent becomes more electron-donating.

Last, an alternative method for the synthesis of $\mathbf{1X_R}$ is via an intermolecular Suzuki–Miyaura cross-coupling. To test this route, $\mathbf{3_{11}}$ and biphenyl-3,3′-diboronic acid bis(pinacol) ester were cross-coupled under dilute conditions (See Supporting Information). The isolated yield of $\mathbf{1a_{11}}$ following this route was 8%. Therefore, the intermolecular approach to nanogloves synthesis is discouraged in favor of the intramolecular Yamamoto coupling.

Structural Analysis

Single-crystal X-ray diffraction confirmed the glove-like structure of $\mathbf{1a_5}$, $\mathbf{1b_{11}}$, and $\mathbf{1c_{11}}$. High-quality single crystals were grown by slowly diffusing MeCN into chlorobenzene solutions of $\mathbf{1a_5}$, $\mathbf{1b_{11}}$, and $\mathbf{1c_{11}}$. In addition to confirming the connectivity of $\mathbf{1a_5}$ (Figure 3), its crystal structure displays a cofacial dimeric nature in the solid state, resulting from noncovalent CH···π interactions (Figure S20). Note that $\mathbf{1b_{11}}$ (Figure S21) and $\mathbf{1c_{11}}$ (Figure S22) have a different packing that does not involve a face-to-face interaction, likely because substituent E prevents dimerization from happening.

The biphenyl moiety defined by rings A and A′ in Figure 3 is relatively planar across $\mathbf{1a_5}$, $\mathbf{1b_{11}}$, and $\mathbf{1c_{11}}$ with dihedral angles of 16(4), 8(3), and 11(6) degrees, respectively. The planarity introduced into this biphenyl moiety is a direct result of the nanoglove architecture. To obtain quantitative information regarding the contraction introduced during nanoglove formation, the centroid of ring B was determined in all structures and the distance to the opposing centroid was extracted from the single-crystal X-ray diffraction data. Precursors $\mathbf{3_5}$ and $\mathbf{2a_5}$ display centroid-to-centroid distances of 12.7(6) and 12.70(5) Å, respectively, while nanogloves $\mathbf{1a_5}$, $\mathbf{1b_5}$, and $\mathbf{1c_{11}}$ exhibit only a small contraction to 11.7(3), 11.7(2), and 11.7(3) Å, respectively. The latter minor structural changes in centroid-to-centroid distance between precursors and nanogloves indicate that rigidification due to macrocyclization should result in an insignificant buildup of strain. In fact, based on the homodesmotic reaction in Figure S25 the strain energy of $\mathbf{1a_1}$ (R = Me) is ~9 kcal mol^{-1} (obtained by DFT at the B3LYP/6-31G(d) level of theory).[57]

Electronic Structure

The absorption and emission properties of nanogloves were investigated in dichloromethane to determine their electronic structure. All three nanogloves $\mathbf{1a_{11}}$, $\mathbf{1b_{11}}$, and $\mathbf{1c_{11}}$ have a well-defined main absorption band in the short-wave ultraviolet region, specifically at λ_{max} of 254, 259, and 253 nm (Figure 4 left), respectively. This main absorption band is independent of the nature of substituent E and matches λ_{max} for benzene (255 nm).[23] This similarity is expected due to destructive quantum interference resulting from the cross-conjugated nature of the twelve phenylene rings forming the outer rim of the nanoglove.[58–60] Additionally, a series of low-energy weak absorption bands are unique in $\mathbf{1c_{11}}$ between 300 and 340 nm, with the lowest energy peak at ~330 nm.

The emission spectra for all three nanogloves $\mathbf{1a_{11}}$, $\mathbf{1b_{11}}$, and $\mathbf{1c_{11}}$ are nearly identical, showing an emission band

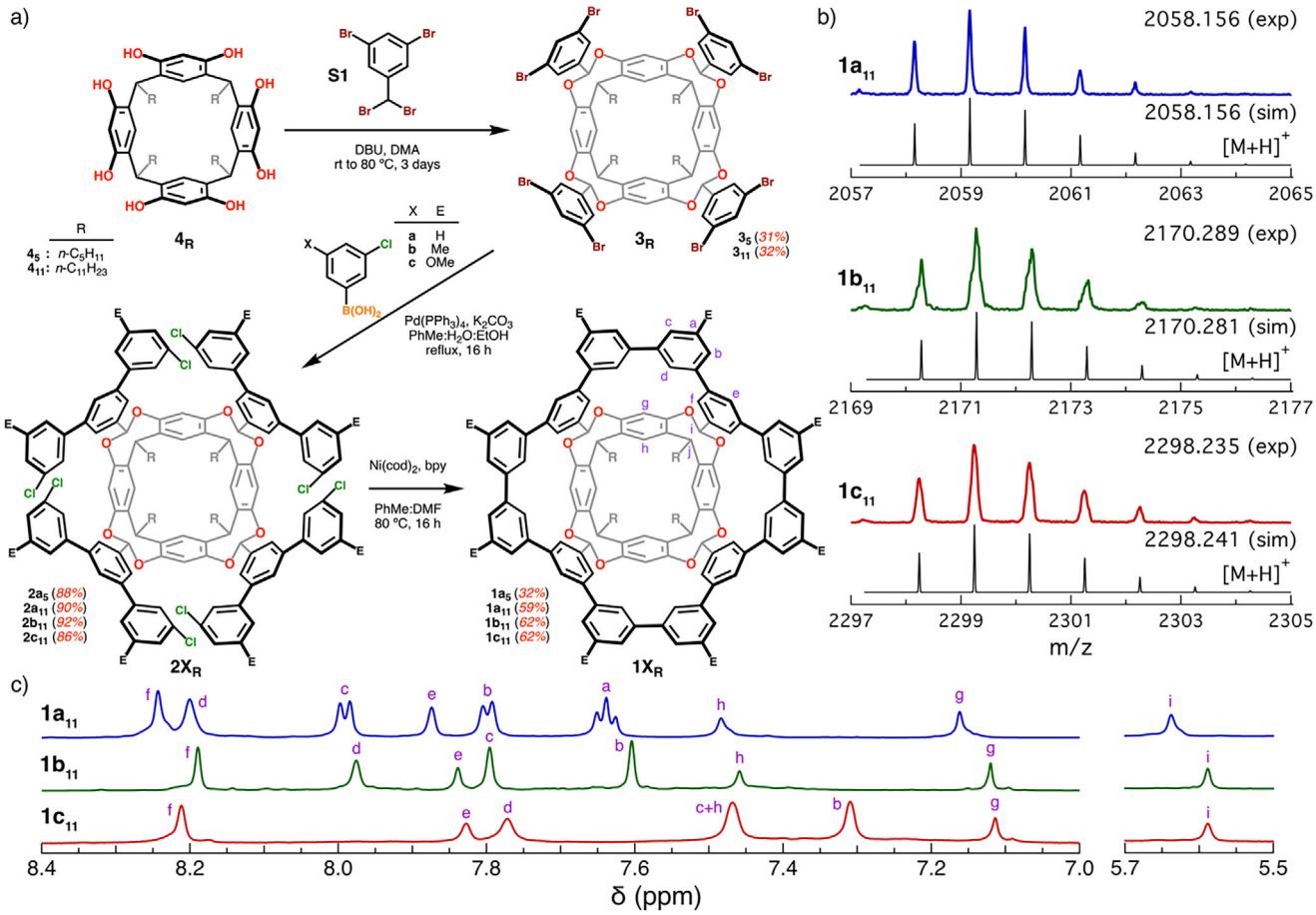

Figure 2. Synthesis and characterization of nanogloves. a) Synthesis of $\mathbf{1X_R}$ starting from resorcin[4]arenes $\mathbf{4_5}$ and $\mathbf{4_{11}}$. b) Experimental MALDI MS molecular ion peaks of $\mathbf{1X_{11}}$. Black traces represent simulations of $[M + H]^+$ isotopic distributions. c) ^{1}H NMR of $\mathbf{1a_{11}}$, $\mathbf{1b_{11}}$, and $\mathbf{1c_{11}}$ in 1,1,2,2-tetrachloroethane-d_2 at 20 °C. Proton labels according to (a). Note: in the synthesis of $\mathbf{2c_{11}}$, boronic acid pinacol ester was used instead of the free boronic acid. $\mathbf{1b_5}$ and $\mathbf{1c_5}$ were not synthesized.

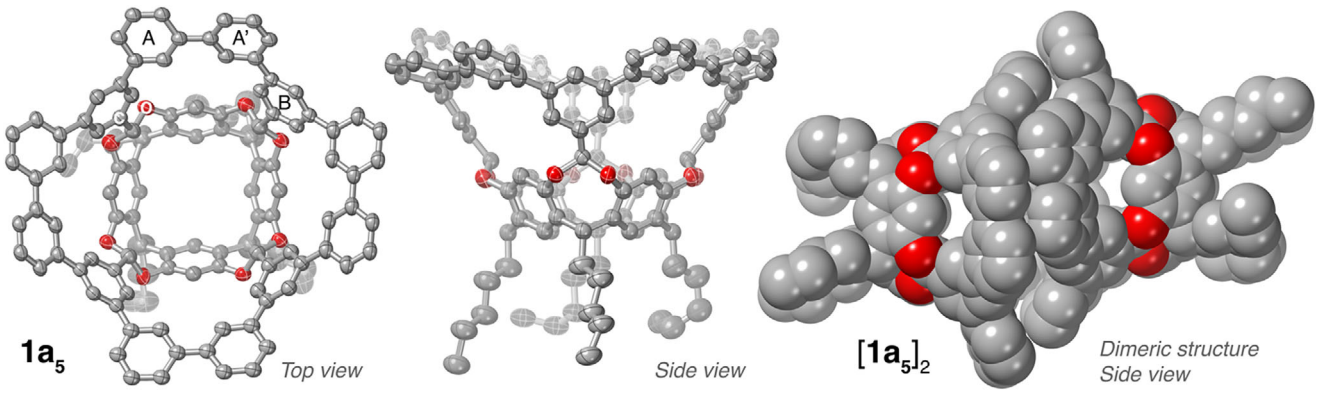

Figure 3. Molecular crystal structure of $\mathbf{1a_5}$ at 120 K. Thermal ellipsoids are shown at 50% probability level. The dimeric structure of $\mathbf{1a_5}$ is shown on the right-hand side in the sphere packing model.

maximum around 342–343 nm (Figure 4 right). Interestingly, a second band is observed for $\mathbf{1c_{11}}$ at 354 nm. Time-dependent (TD) DFT calculations were used to investigate the nature of these electronic transitions. The major absorption bands are reproduced, albeit shifted to lower energies. For instance, major transitions around 280–300 nm were found in model compounds $\mathbf{1a_1}$ (282 nm, oscillator strength $= f \approx 0.27$), $\mathbf{1b_1}$ (285 nm, $f \approx 0.33$), and $\mathbf{1c_1}$ (299 nm, $f \approx 0.30$). A low-energy transition in $\mathbf{1c_1}$ at 314 nm is calculated to correspond to $H \rightarrow L + 2$, which is attributed to one of the low-energy bands observed in this compound (Table S2). In contrast to our previous reports[50,51] and [*n*]cyclo-*para*-phenylenes,[61,62] the

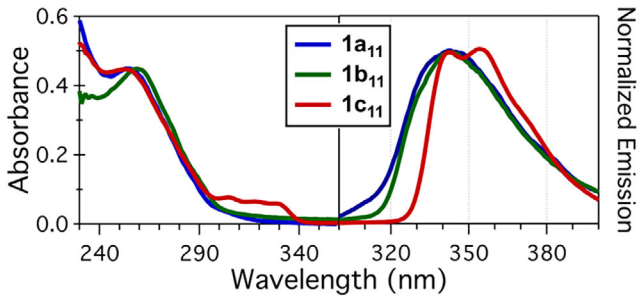

Figure 4. (*Left*) Absorption and (*right*) emission bands of nanogloves **1X$_{11}$** collected in CH_2Cl_2 at room temperature.

HOMO-to-LUMO transition is not forbidden in nanogloves. For example, in **1a$_1$** the transition around 288 nm ($f \approx 0.04$) has a 55% contribution from the HOMO-to-LUMO transition, and similarly for **1b$_1$** and **1c$_1$** at 289 ($f \approx 0.07$, 64%) and 294 nm ($f \approx 0.05$, 34%), respectively.

To understand why the HOMO-to-LUMO transition is not forbidden, as it is in other conjugated macrocycles,[63] we evaluated the frontier molecular orbitals (FMOs) of nanogloves. The HOMO and LUMO for **1a$_1$**, **1b$_1$**, and **1c$_1$** are depicted in Figures S27 to S29, respectively. In contrast to [*n*]CPPs, where the HOMO and LUMO reside uniformly across the conjugated nanoring,[64] qualitatively the HOMO and LUMO are not evenly distributed across the [12]CMP fragment of the nanoglove. In fact, the uneven orbital distribution is more apparent as the electron donating ability increases in substituent E. Analysis of the HOMO of **1a$_1$** and **1b$_1$** showcases a benzenoid character in the biphenyl fragment composed of rings A and A′ (Figure 3), while **1c$_1$** resembles more of a quinoidal shape.

Catching Fullerenes

Fullerenes have a unique spheroidal π–conjugated surface. Receptors for fullerenes capable of establishing host:guest (H:G) adducts have been explored since the discovery of C_{60}.[65] A non-exhaustive list of fullerene receptors includes molecular tweezers,[66–68] carbon nanohoops,[69,70] phenine nanotubes,[71] metallosupramolecular receptors,[72,73] (metallo)porphyrins,[74–78] molecular organic cages,[79–81] corannulene hosts,[82] adaptable macrocycles,[83] calix[*n*]arenes,[84,85] cavitands,[86,87] and metal-organic frameworks.[88,89] Most of these hosts stabilize fullerenes through concave-convex π–π interactions.[90–92] Almost all of the previous receptors were purposely designed to bind fullerenes; however, some macrocyclic arenes, like those introduced earlier in this manuscript, have been found to encapsulate fullerenes due to their basket-like structure. Examples include cyclotriveratrylene (CTV),[93,94] calix[*n*]arenes,[95,96] and pillar[*n*]arenes.[97] Most of these macrocycles display weak binding towards fullerenes in solution ($<10^3$ M^{-1})[97] or they only form adducts in the solid state by benefiting from their size complementarity.[98,99] Most relevant, molecules with spherical or pseudospherical geometries able to encapsulate C_{60} are rare.[100,101]

We hypothesized that their bowl-shaped structure would give nanogloves the ability to host fullerenes. The binding affinity of C_{60} for **1a$_{11}$** was tested using ^{1}H NMR in 1,1,2,2-tetrachloroethane-d_2 (TeCA-d_2). The NMR solvent was chosen to maximize the solubility of C_{60},[102] while maintaining **1a$_{11}$** in solution. Upon titration of C_{60} into **1a$_{11}$**, the resonance of the acetal hydrogen, labeled as "i", shifted from 5.62 to 5.41 ppm (Figure 5a), while methine resonance "j" shifts only by a tenth of a ppm downfield, remaining at around 5.07 ppm. Most interestingly, a minor new set of acetal (4.84 ppm) and methine (4.81 ppm) resonances appear and disappear as the titration proceeds forward, maximizing at ~0.5 equivalents of C_{60} (Figure S30). As the titration proceeds, free **1a$_{11}$** and these new sets of resonances co-exist; therefore, the equilibrium established during adduct formation strongly favors the host-guest complex species with an association constant (K_a) surpassing the limit measurable by NMR ($>10^6$ M^{-1}).[103] Free **1a$_{11}$** and the set of resonances at ~4.8 ppm essentially disappear at one or more equivalents of C_{60}. Analysis of this data led us to hypothesize that the adduct at ~5.41 ppm is likely the 1:1 H:G species $C_{60}\subset$**1a$_{11}$**, which predominates over the 2:1 H:G $C_{60}\subset$(**1a$_{11}$**)$_2$ complex at ~4.8 ppm. Observing that resonance "i" shifts upfield, we find literature reports indicating that aromatic C–H bonds move upfield as π–π stacking increases.[104,105] However, in our case, it is an acetal C–H bond pointing at C_{60}. Computational studies indicate a shielding effect above the hexagonal rings in C_{60} and C_{70}, and deshielding when above the pentagons.[106] Previous reports show a net deshielding effect,[107] while in our case a net shielding of the acetal C–H is observed. Furthermore, titration experiments of C_{60} into **1b$_{11}$** (Figure S31) or **1c$_{11}$** (Figure S32) display the formation of only the 1:1 H:G species at exactly one equivalent of C_{60} and complete absence of the putative 2:1 H:G compound.

Titration experiments involving C_{70} presented an additional intricacy. As shown in Figure 5b, titration of C_{70} into **1a$_{11}$** produces a mixture of two host-guest adducts. One adduct with acetal ("i") and methine ("j") resonances at 5.43 and 4.99 ppm, respectively, and a second minor species displaying an acetal resonance at 5.76 ppm and methine peak at 5.16 ppm. Note that at one equivalent of C_{70} both adducts persist; assignment of the 1:1 and 2:1 H:G species is challenging solely based on this data. Interestingly, when C_{70} is titrated to **1b$_{11}$** (Figure S34) or **1c$_{11}$** (Figure S35) the downfield shifted adduct is the only one observed, concomitantly the nanoglove's resonances fully disappear with the addition of one equivalent of C_{70}. Tentatively, these data suggest that the downfield-shifted resonances in all three cases of C_{70} into **1X$_{11}$** correspond to the 1:1 H:G species $C_{70}\subset$**1X$_{11}$**. Therefore, the adduct with upfield-shifted peaks in the titration experiment using **1a$_{11}$** is likely the 2:1 H:G complex $C_{70}\subset$(**1a$_{11}$**)$_2$. As noted above, the SCXRD data for **1b$_{11}$** and **1c$_{11}$** do not show cofacial interactions, hinting at the unlikelihood of dimer formation, hence the absence of upfield-shifted acetal resonances. The spectrum labeled "VT" in Figure 5b was subjected to variable-temperature ^{1}H NMR to determine whether the two adducts coalesce into one and whether there is a preference for one over the other. Data collected up to 85 °C showcases how the resonances for the

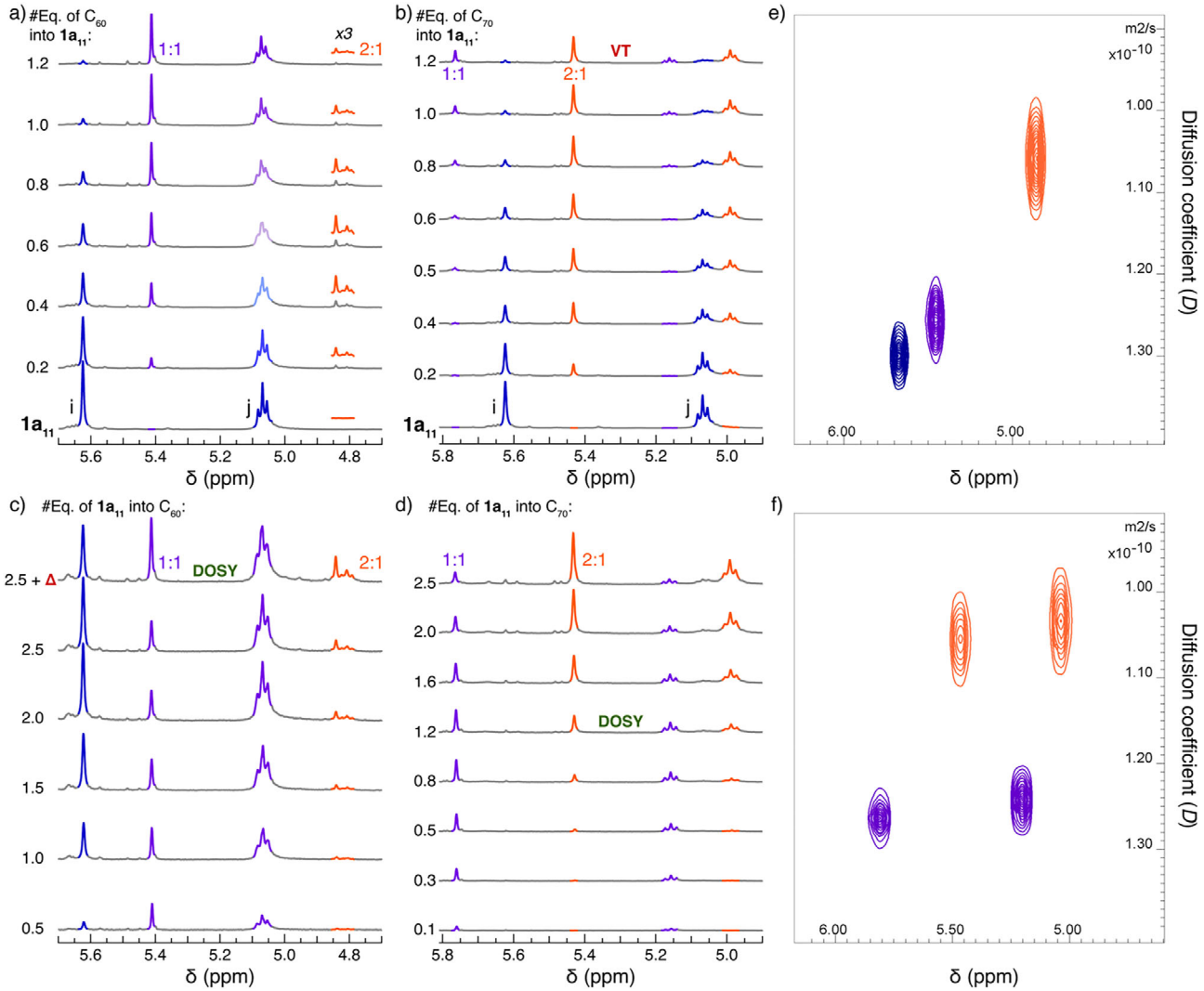

Figure 5. Fullerene binding to nanogloves and diffusion of nanoglove-fullerene adducts. ^{1}H NMR titration experiments: a) C_{60} into **1a$_{11}$**, and b) C_{70} into **1a$_{11}$**; and reverse titrations: c) **1a$_{11}$** into C_{60}, and d) **1a$_{11}$** into C_{70}. The 1:1 and 2:1 H:G adducts are highlighted in purple and orange traces, respectively. Resonances "i" and "j" are labeled according to Figure 2. Spectrum of the sample labeled with "VT" in (b) was employed in variable-temperature experiments. Spectra in (c) and (d) marked with the "DOSY" label were used for DOSY NMR experiments shown in (e) and (f). The top spectrum in (c) was heated to reflux for 5 min. DOSY NMR data: e) Select resonances showcasing the diffusion of **1a$_{11}$** (blue trace), 1:1 H:G adduct $C_{60}\subset$**1a$_{11}$** (purple trace), and 2:1 H:G adduct $C_{60}\subset$(**1a$_{11}$**)$_2$ (orange trace). f) Select resonances indicating the 1:1 H:G adduct $C_{70}\subset$**1a$_{11}$** (purple trace), and 2:1 H:G adduct $C_{70}\subset$(**1a$_{11}$**)$_2$ (orange trace). The region of the acetal and methine resonances "i" and "j", respectively, are shown in the DOSY NMR data. All ^{1}H NMR titrations and DOSY NMR data were performed in 1,1,2,2-tetrachloroethane-d_2 (TeCA-d_2) at 20 °C.

2:1 H:G species remain sharp while the 1:1 H:G complex broadens (Figure S36). The broadening effect is associated with decreased affinity between the host and the guest at high temperature. Altogether, the data indicates the adduct $C_{70}\subset$(**1a$_{11}$**)$_2$ is relatively more stable than $C_{70}\subset$**1a$_{11}$**; however, both species maintain their composition up to 85 °C.

To clarify the assignment of 1:1 and 2:1 H:G adducts, reverse titration experiments were conducted by adding **1a$_{11}$** into fullerenes. Figure 5c demonstrates that the reverse titration of **1a$_{11}$** into C_{60} preferentially forms the 1:1 H:G adduct over the 2:1 H:G species, and only a small amount of the 2:1 complex is formed after heating the solution to reflux. Note that although C_{60} is soluble in TeCA, its solubility is not high enough to allow for all C_{60} to be dissolved in the titration experiment shown in Figure 5c, thus some C_{60} remains as precipitate in the NMR tube. Titration of **1a$_{11}$** into C_{70} shows initial formation of the 1:1 H:G adduct, which experiences a monotonic decrease as equivalents of **1a$_{11}$** reach ~0.5 equivalents, at which point the 2:1 H:G species begins to form (Figure 5d).

The nuclearity of the H:G adducts determines their overall hydrodynamic radii, and therefore their diffusive properties in solution. We hypothesize that the diffusion coefficient (D) of the 1:1 versus 2:1 H:G adducts will provide conclusive evidence to support their assignment. Typically, D is determined through DOSY NMR spectroscopy.[108] For reference, D for C_{60} and C_{70} has been determined in a variety of solvents with different viscosities (η) and it ranges from 1to9 × 10^{-10} m^2 s^{-1}.[109] Specifically, D for C_{60} in *o*-DCB (η = 1.32) and benzonitrile (η = 1.24) is 1.1(2) × 10^{-10}

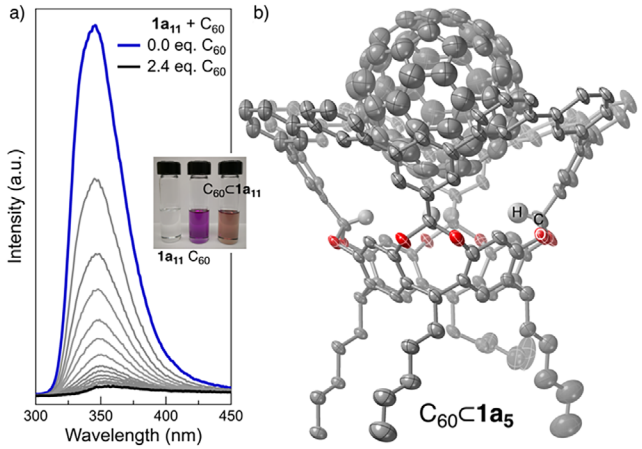

Figure 6. a) Fluorescence quenching titration of $\mathbf{1a_{11}}$ with C_{60} in TeCA at room temperature. Inset: photographic images of solutions of $\mathbf{1a_{11}}$, C_{60}, and $C_{60}\subset\mathbf{1a_{11}}$ in TeCA under ambient light. b) Molecular crystal structure of $C_{60}\subset\mathbf{1a_5}$ at 100 K. Thermal ellipsoids are shown at 50% probability level. C and O are shown in grey and red, respectively.

and $1.4(3) \times 10^{-10}$ m^2 s^{-1}, respectively, which we assume to be close to that in TeCA ($\eta = 1.43$) based on their similar viscosity properties.[110] In H:G complexes, DOSY NMR can only be reliably applied to adducts existing in the slow exchange regime,[111] which is the case here as established in Figure 5a–d. To this end, we examined the top spectrum in Figure 5c via DOSY NMR. We provide the zoomed in part of the DOSY NMR in Figure 5e where we expect to find free $\mathbf{1a_{11}}$ and the previously assigned 1:1 and 2:1 H:G adducts. All three species showed different D values. For instance, $\mathbf{1a_{11}}$ displays $D = 1.31(1) \times 10^{-10}$ m^2 s^{-1}, $C_{60}\subset\mathbf{1a_{11}}$ results in D of $1.26(2) \times 10^{-10}$ m^2 s^{-1}, and $C_{60}\subset(\mathbf{1a_{11}})_2$ comes behind at $1.06(3) \times 10^{-10}$ m^2 s^{-1}. Similarly, DOSY NMR data of a sample containing roughly equimolar amounts of $C_{70}\subset\mathbf{1a_{11}}$ and $C_{70}\subset(\mathbf{1a_{11}})_2$ results in D of $1.25(1) \times 10^{-10}$ and $1.05(1) \times 10^{-10}$ m^2 s^{-1} (Figure 5f), respectively. Overall, DOSY NMR data corroborates the assignment of the 1:1 and 2:1 H:G adducts and demonstrate that their diffusion properties are independent of the hosted fullerene and are only influenced by the adduct's nuclearity or size. Notably, the size difference between the 1:1 adducts is rather small and is not reflected in different D values; however, comparing the 1:1 versus the 2:1 H:G species for either C_{60} or C_{70} results in a measurable size increase that is reflected in the lower D values for the 2:1 H:G adducts. For reference, the adduct $C_{60}\subset(\mathbf{1a_1})_2$ is larger than $C_{60}\subset\mathbf{1a_1}$ (Figure S38), and the same is true for adducts of C_{70} (Figure S39), which inevitably impact their hydrodynamic radius and as a result their diffusivity. These findings follow expected trends obtained by others correlating D with molecular weight.[112,113]

Intrigued by the strong binding of fullerenes to nanogloves, we obtained quantitative binding data by carrying out fluorescence quenching experiments. A representative example is shown in Figure 6a, where C_{60} is titrated to $\mathbf{1a_{11}}$ and the evolution of the emission band at 342 nm is recorded as titration proceeds from 0 to 2.4 equivalents of C_{60}. All titration experiments of C_{60} and C_{70} into $\mathbf{1X_{11}}$ are shown in Figures S40 to S42. All data were analyzed using Bindfit[114] for a 1:1 H:G model, except the titration of C_{70} into $\mathbf{1a_{11}}$, which is best described by a 2:1 H:G adduct formation (Figure 5b). Interestingly, K_a values across all five titrations following a 1:1 H:G model for C_{60} and C_{70} into $\mathbf{1X_{11}}$ fluctuate around 1-to-3 $\times$ 10^7 M^{-1} in TeCA at room temperature. Titration of C_{70} into $\mathbf{1a_{11}}$ was best fit by K_{11} and K_{21} of 1.5×10^5 and 2.0×10^6 M^{-1}, respectively. The strong fullerene association observed within nanogloves is larger or comparable to the strongest host:fullerene adducts reported in the literature.[72,115–117] Qualitatively, C_{60} encapsulation can be readily detected with the naked eye as the colorless host solution of $\mathbf{1a_{11}}$ changes to brown with incremental addition of the purple solution of C_{60} (Figure 6a inset). Strong binding of fullerenes facilitated the formation of high-quality single crystals by slow diffusion of MeCN into $C_{60}\subset\mathbf{1a_5}$ in *ortho*-dichlorobenzene (*o*-DCB). The molecular crystal structure of $C_{60}\subset\mathbf{1a_5}$ displays the fullerene perfectly nested within the nanoglove (Figures 6b and S43). The average distance between the acetal hydrogen and the closest carbon atom at C_{60} is 2.91(3) Å. This short distance indicates a strong C–H•••π interaction according to literature values.[118] Moreover, π–π interactions are also operative as determined from the short average distance of 3.31(7) Å between the centroid of ring B (Figure 3) and the closest carbon atom or ring centroid at C_{60}.[119] DFT calculations using the independent gradient model based on Hirshfeld partition of molecular density (IGMH) provide a visualization of the non-covalent interaction surface between C_{60} and $\mathbf{1a_1}$ (Figure S44).[120] The bowl-shape of this interaction surface demonstrates the excellent nesting pocket provided by nanogloves $\mathbf{1X_{11}}$. Last, the overall geometry of $\mathbf{1a_5}$ remains unchanged upon host-guest adduct formation, suggesting a negligible penalty in reorganizational energy, thus resulting in enhanced binding affinity constants.[121,122]

Expanding Fullerene Recognition

Fullerene availability is hindered by challenging separation and purification procedures.[123,124] Fullerene-rich carbon soots (CSs) are available commercially, containing ~5% fullerenes.[125] However, additional information about the specific composition of fullerenes present, aside from C_{60} and C_{70}, is not disclosed or well-known. We hypothesized that fullerenes in general may bind to nanogloves even if they were present in complex mixtures. To test this hypothesis, CS was suspended in a solution of $\mathbf{1a_{11}}$ in TeCA at 100 °C for 12 h (detailed procedure in Supporting Information). The suspension was filtered, and the resulting solution was dried under reduced pressure. Since the acetal and methine resonances "i" and "j", respectively, are sensitive to the formation of fullerene⊂nanoglove adducts, the filtrate was subjected to ^{1}H NMR analysis in TeCA-d_2 to search for potential fullerene complexes. The region of the ^{1}H NMR spectrum from 4.7 to 5.8 ppm displays multiple resonances, suggesting a variety of fullerene adducts (Figure S48). The major resonances coincide with $C_{60}\subset\mathbf{1a_{11}}$ and $C_{70}\subset(\mathbf{1a_{11}})_2$; however, several more are discernible that are not related to adducts of C_{60} or C_{70}. Furthermore, analysis of the CS

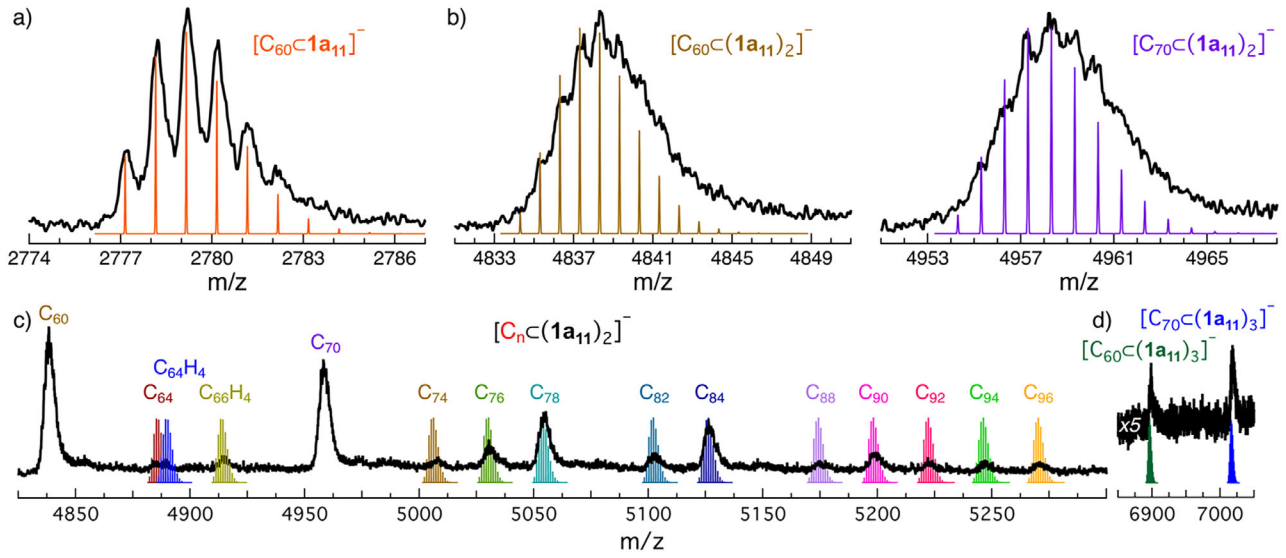

Figure 7. MALDI MS of filtrate after suspending carbon soot (CS) with $\mathbf{1a_{11}}$ in TeCA at 100 °C. Sections of mass spectra displaying (a) the 1:1 H:G adduct $[C_{60}\subset\mathbf{1a_{11}}]^-$, (b) species $[C_{60}\subset(\mathbf{1a_{11}})_2]^-$ and $[C_{70}\subset(\mathbf{1a_{11}})_2]^-$, (c) the region of the spectrum for 2:1 H:G adducts described by $[C_n\subset(\mathbf{1a_{11}})_2]^-$, and (d) identification of the 3:1 H:G for C_{60} and C_{70}, $[C_n\subset(\mathbf{1a_{11}})_3]^-$.

filtrate by DOSY NMR (Figure S49) suggests the formation of 1:1 and 2:1 H:G adducts. Last, despite observing multiple fullerene adducts via NMR their exact molecular identity was not established.

MALDI MS was used to identify the fullerenes obtained from carbon soot. We collected data up to $m/z = 9000$ showing three distinct m/z regions: the first one near 3000, a second one in and around 5000, and a third one at 7000 (Figure S50a). Note that free $\mathbf{1a_{11}}$ is not observed ($m/z = 2058$, Figure 2b). Rather surprisingly, the first region only displays a single species corresponding to $[C_{60}\subset\mathbf{1a_{11}}]^-$ (Figure 7a). In contrast, the second region contains a multitude of ion peaks corresponding to 2:1 H:G adducts, where the major ones match $[C_{60}\subset(\mathbf{1a_{11}})_2]^-$ and $[C_{70}\subset(\mathbf{1a_{11}})_2]^-$ (Figure 7b). Detailed analysis of the minor ion peak distributions between $m/z = 4850$ and 5300 reveals the formation of $[C_n\subset(\mathbf{1a_{11}})_2]^-$ for n = 64, 66, 74, 76, 78, and 82 to 96 every two units, except for 86 (Figure 7c). Note that while most of these adducts match their isotopic distribution considering C_n alone, others are off by several units indicating potential fullerene functionalization. Recently, Yamada, Akasaka, and Nagase highlighted that anomalous carbon cages are present in carbon soot.[126] Aside from C_{60} and C_{70}, using nanoglove $\mathbf{1a_{11}}$ we observe the adduct $[C_n\subset(\mathbf{1a_{11}})_2]^-$ with C_{64} and a closely related species best described as $C_{64}H_4$. Aside from its allotropic form, C_{64} has been isolated as $C_{64}H_4$,[127] $C_{64}Cl_4$,[128] or $C_{64}Cl_8$;[129] similarly, C_{66} alone is not observed, instead data fits better to $C_{66}H_4$.[130] The last two species in the series, C_{74}, C_{76}, and C_{78}, match well to the pure allotrope sandwiched between two nanogloves; however, the experimental pattern does not fit entirely well for $[C_{74}\subset(\mathbf{1a_{11}})_2]^-$, likely indicating an unknown C_{74} cage. Functionalization precedents for these three species are known in the form of $C_{74}Cl_{10}$,[131] $C_{76}Cl_{18}$,[132] $C_{76}Cl_{24}$,[133] and $C_{78}Cl_{18}$.[134] The H:G compound $[C_{80}\subset(\mathbf{1a_{11}})_2]^-$ is not observed in the mass spectrum in Figure 7c. Its absence is not entirely surprising as it is known to exist in low abundance in soot.[135] Fullerene C_{82} and C_{84} match well the simulated isotopic pattern for $[(C_{82}$ or $C_{84})\subset(\mathbf{1a_{11}})_2]^-$. In contrast, C_{86} is absent and C_{88} is barely noticeable in the mass spectrum despite having several stable isomers.[136–138] Fullerene C_{90}, and larger, have been reported to adopt tubular-like structures,[139] and more recently categorized as fullertubes.[140,141] Our data do not allow us to discern the nature of the isomer(s) extracted from CS; however, based on data presented vide supra, isomers with end-caps having C_{60}-like structures will nest better within $\mathbf{1a_{11}}$ and form favorable H:G adducts. Furthermore, the simulated isotopic patterns for $[C_n\subset(\mathbf{1a_{11}})_2]^-$ with C_{92}, C_{94}, and C_{96}[142] match the experimental MS data well. Finally, the third region at around $m/z = 7000$ shows ion peaks matching the adducts $[C_n\subset(\mathbf{1a_{11}})_3]^-$ for C_{60} and C_{70} (Figure 7d). This is somewhat unexpected and suggests the third equivalent of $\mathbf{1a_{11}}$ probably wraps around the ternary adduct $[C_n\subset(\mathbf{1a_{11}})_2]^-$ as a stitch. Finally, comparing mass spectra data of CS in the presence and absence of nanogloves demonstrates preferential detection of fullerenes when $\mathbf{1a_{11}}$ is present, especially for congeners heavier than C_{70} (Figure S51).

Conclusion

Following on our synthetic strategy to make contorted aromatic species, here we report the efficient access to molecules with deep cavities coined nanogloves. Employing resorcin[4]arene as the template, and two subsequent coupling reactions, we disclose a series of nanogloves with exceptional binding affinities for buckyballs. The top rim represents a [12]CMP structure, which is covalently linked to the template via four benzal C—C bonds. The high binding constants of fullerenes to nanogloves are attributed to their rigid structure, allowing them to establish a surface of non-covalent $\pi\cdots\pi$ contacts and CH$\cdots\pi$ interactions with the

nested buckyball. Moreover, we exploit fullerene's high binding affinities towards nanogloves to selectively sequester and detect them from carbon soot. This work may lead the way to the synthesis of unprecedented structures and materials to use in fullerene purification, their regioselective functionalization, and fullerene solubilization for their availability in standard organic solvents.

Supporting Information

The authors have cited additional references within the Supporting Information (Ref.[23,53–56,103,120,143–159]).

Acknowledgements

This research was partially supported by the National Science Foundation NSF CAREER CHE-2302628. This research was supported with startup funds by Rice University and the University of Pittsburgh. The authors thank Dr. Christopher L. Pennington for assistance with HRMS data collection. R.H.S. acknowledges the support of the Robert A. Welch Foundation Young Investigator Award. S.M. acknowledges the support from the Dietrich School of Arts & Sciences Graduate Fellowship and the Andrew Mellon Pre-doctoral Fellowship. This research was funded in part by a grant from the Welch Foundation (C-2142-20230405). NSF's ChemMatCARS, Sector 15 at the Advanced Photon Source (APS), Argonne National Laboratory (ANL) is supported by the Divisions of Chemistry (CHE) and Materials Research (DMR), National Science Foundation, under grant number NSF/CHE-1834750 and NSF/CHE-2335833 This research used resources of the Advanced Photon Source; a U.S. Department of Energy (DOE) Office of Science user facility operated for the DOE Office of Science by Argonne National Laboratory under Contract No. DE-AC02-06CH11357. The authors thank the support from the Center for Research Computing at Rice University and the University of Pittsburgh. This research was supported through instrumentation made available through the Shared Equipment Authority at Rice University.

Conflict of Interests

The authors declare no conflict of interest.

Data Availability Statement

The data that support the findings of this study are available from the corresponding author upon reasonable request.

Keywords: [12]cyclo-*meta*-phenylene • Curved cavitands • Fullerene host • Nanoglove • Synthetic receptors

[1] M. Iyoda, J. Yamakawa, M. J. Rahman, *Angew. Chem. Int. Ed.* **2011**, *50*, 10522–10553.
[2] L. Zang, Y. Che, J. S. Moore, *Acc. Chem. Res.* **2008**, *41*, 1596–1608.
[3] E. J. Leonhardt, R. Jasti, *Nat. Rev. Chem.* **2019**, *3*, 672–686.
[4] D. Lu, Q. Huang, S. Wang, J. Wang, P. Huang, P. Du, *Front. Chem.* **2019**, *7*, 668.
[5] Q. Duan, F. Wang, K. Lu, *Front. Chem.* **2022**, *10*, 973313.
[6] X. Li, Y. Jin, N. Zhu, J. Yin, L. Y. Jin, *Sensors* **2024**, *24*, 1530.
[7] M. Ball, B. Zhang, Y. Zhong, B. Fowler, S. Xiao, F. Ng, M. Steigerwald, C. Nuckolls, *Acc. Chem. Res.* **2019**, *52*, 1068–1078.
[8] H. Zhang, X. Ma, K. T. Nguyen, Y. Zhao, *ACS Nano* **2013**, *7*, 7853–7863.
[9] C. Sathiyajith, R. R. Shaikh, Q. Han, Y. Zhang, K. Meguellati, Y.-W. Yang, *Chem. Commun.* **2017**, *53*, 677–696.
[10] X.-N. Han, Y. Han, C.-F. Chen, *Chem. Soc. Rev.* **2023**, *52*, 3265–3298.
[11] W. S. Rapson, R. G. Shuttleworth, J. N. van Niekerk, *J. Chem. Soc.* **1943**, 326–327.
[12] I. L. Karle, L. O. Brockway, *J. Am. Chem. Soc.* **1944**, *66*, 1974–1979.
[13] L. Ernst, A. Mannschreck, K.-D. Rümpler, *Org. Magn. Reson.* **1973**, *5*, 125–128.
[14] E. Wuckert, C. Hägele, F. Giesselmann, A. Baro, S. Laschat, *Beilstein J. Org. Chem.* **2009**, *5*, 57.
[15] H. Huang, C.-K. Hau, C. C. M. Law, H. N. C. Wong, *Org. Biomol. Chem.* **2009**, *7*, 1249–1257.
[16] A. Rajca, S. Rajca, *Angew. Chem. Int. Ed.* **2010**, *49*, 672–674.
[17] H. A. Staab, F. Binnig, *Tetrahedron Lett.* **1964**, *5*, 319–321.
[18] H. A. Staab, F. Binnig, *Chem. Ber.* **1967**, *100*, 293–305.
[19] D. J. Cram, T. Kaneda, R. C. Helgeson, G. M. Lein, *J. Am. Chem. Soc.* **1979**, *101*, 6752–6754.
[20] D. J. Cram, T. Kaneda, R. C. Helgeson, S. B. Brown, C. B. Knobler, E. Maverick, K. N. Trueblood, *J. Am. Chem. Soc.* **1985**, *107*, 3645–3657.
[21] W. Pisula, M. Kastler, C. Yang, V. Enkelmann, K. Müllen, *Chem. Asian J.* **2007**, *2*, 51–56.
[22] J. M. W. Chan, T. M. Swager, *Tetrahedron Lett.* **2008**, *49*, 4912–4914.
[23] J. Y. Xue, K. Ikemoto, N. Takahashi, T. Izumi, H. Taka, H. Kita, S. Sato, H. Isobe, *J. Org. Chem.* **2014**, *79*, 9735–9739.
[24] R. Jasti, J. Bhattacharjee, J. B. Neaton, C. R. Bertozzi, *J. Am. Chem. Soc.* **2008**, *130*, 17646–17647.
[25] S. E. Lewis, *Chem. Soc. Rev.* **2015**, *44*, 2221–2304.
[26] T. C. Lovell, C. E. Colwell, Lev N. Zakharov, R. Jasti, *Chem. Sci.* **2019**, *10*, 3786–3790.
[27] T. C. Lovell, S. G. Bolton, J. P. Kenison, J. Shangguan, C. E. Otteson, F. Civitci, X. Nan, M. D. Pluth, R. Jasti, *ACS Nano* **2021**, *15*, 15285–15293.
[28] H. M. Bergman, G. R. Kiel, R. C. Handford, Y. Liu, T. D. Tilley, *J. Am. Chem. Soc.* **2021**, *143*, 8619–8624.
[29] J. Zhu, Y. Han, Y. Ni, G. Li, J. Wu, *J. Am. Chem. Soc.* **2021**, *143*, 2716–2721.
[30] Y. Li, H. Kono, T. Maekawa, Y. Segawa, A. Yagi, K. Itami, *Acc. Mater. Res.* **2021**, *2*, 681–691.
[31] Y. Segawa, T. Watanabe, K. Yamanoue, M. Kuwayama, K. Watanabe, J. Pirillo, Y. Hijikata, K. Itami, *Nature Synth*. **2022**, *1*, 535–541.
[32] S. Nishigaki, Y. Shibata, A. Nakajima, H. Okajima, Y. Masumoto, T. Osawa, A. Muranaka, H. Sugiyama, A. Horikawa, H. Uekusa, H. Koshino, M. Uchiyama, A. Sakamoto, K. Tanaka, *J. Am. Chem. Soc.* **2019**, *141*, 14955–14960.
[33] G. Naulet, L. Sturm, A. Robert, P. Dechambenoit, F. Röhricht, R. Herges, H. Bock, F. Durola, *Chem. Sci.* **2018**, *9*, 8930–8936.
[34] W. Fan, T. Matsuno, Y. Han, X. Wang, Q. Zhou, H. Isobe, J. Wu, *J. Am. Chem. Soc.* **2021**, *143*, 15924–15929.
[35] Q.-H. Guo, Y. Qiu, M.-X. Wang, J. Fraser Stoddart, *Nat. Chem.* **2021**, *13*, 402–419.

[36] M. Krzeszewski, H. Ito, K. Itami, *J. Am. Chem. Soc.* **2022**, *144*, 862–871.
[37] C. J. White, A. K. Yudin, *Nat. Chem.* **2011**, *3*, 509–524.
[38] J.-R. Wu, Y.-W. Yang, *Chem. Commun.* **2019**, *55*, 1533–1543.
[39] Y. Li, Y. Segawa, A. Yagi, K. Itami, *J. Am. Chem. Soc.* **2020**, *142*, 12850–12856.
[40] N. Kai, H. Kono, A. Yagi, K. Itami, *Synlett* **2023**, *34*, 1433–1436.
[41] H. Kono, Y. Li, R. Zanasi, G. Monaco, F. F. Summa, L. T. Scott, A. Yagi, K. Itami, *J. Am. Chem. Soc.* **2023**, *145*, 8939–8946.
[42] X.-S. Du, D.-W. Zhang, Y. Guo, J. Li, Y. Han, C.-F. Chen, *Angew. Chem. Int. Ed.* **2021**, *60*, 13021–13028.
[43] F. Zhang, X.-S. Du, D.-W. Zhang, Y.-F. Wang, H.-Y. Lu, C.-F. Chen, *Angew. Chem. Int. Ed.* **2021**, *60*, 15291–15295.
[44] Q. Zhang, Y.-E. Zhang, S. Tong, M.-X. Wang, *J. Am. Chem. Soc.* **2020**, *142*, 1196–1199.
[45] J. N. Smith, N. T. Lucas, *Chem. Commun.* **2018**, *54*, 4716–4719.
[46] E. André, B. Boutonnet, P. Charles, C. Martini, J.-M. Aguiar-Hualde, S. Latil, V. Guérineau, K. Hammad, P. Ray, R. Guillot, V. Huc, *Chem. - Eur. J.* **2016**, *22*, 3105–3114.
[47] P. Della Sala, C. Talotta, A. Capobianco, A. Soriente, M. De Rosa, P. Neri, C. Gaeta, *Org. Lett.* **2018**, *20*, 7415–7418.
[48] R. Frydrych, T. Lis, W. Bury, J. Cybińska, M. Stępień, *J. Am. Chem. Soc.* **2020**, *142*, 15604–15613.
[49] A. Nasser Moussa Bamba, A. Ben Saida, I. Abdellah, S. Latil, V. Guérineau, J.-F. Gallard, V. Huc, *Eur. J. Org. Chem.* **2024**, *27*, e202400485.
[50] S. Mirzaei, E. Castro, R. H. Sánchez, *Chem. Sci.* **2020**, *11*, 8089–8094.
[51] E. Castro, S. Mirzaei, R. H. Sánchez, *Org. Lett.* **2021**, *23*, 87–92.
[52] G. Fan, Z. Zhang, G. Wang, L. Shao, B. Hua, F. Huang, *Chem. Sci.* **2024**, *15*, 10713–10723.
[53] L. M. Tunstad, J. A. Tucker, E. Dalcanale, J. Weiser, J. A. Bryant, J. C. Sherman, R. C. Helgeson, C. B. Knobler, D. J. Cram, *J. Org. Chem.* **1989**, *54*, 1305–1312.
[54] S. Merget, L. Catti, G. Piccini, K. Tiefenbacher, *J. Am. Chem. Soc.* **2020**, *142*, 4400–4410.
[55] M. B. Hillyer, C. L. D. Gibb, P. Sokkalingam, J. H. Jordan, S. E. Ioup, B. C. Gibb, *Org. Lett.* **2016**, *18*, 4048–4051.
[56] K. Srinivasan, B. C. Gibb, *Org. Lett.* **2007**, *9*, 745–748.
[57] A. D. Becke, *J. Chem. Phys.* **1993**, *98*, 5648–5652.
[58] N. F. Phelan, M. Orchin, *J. Chem. Educ.* **1968**, *45*, 633.
[59] P. A. Limacher, H. P. Lüthi, *WIREs Comput. Mol. Sci.* **2011**, *1*, 477–486.
[60] H. Valkenier, C. M. Guédon, T. Markussen, K. S. Thygesen, S. J. van der Molen, J. C. Hummelen, *Phys. Chem. Chem. Phys.* **2014**, *16*, 653–662.
[61] T. Nishihara, Y. Segawa, K. Itami, Y. Kanemitsu, *J. Phys. Chem. Lett.* **2012**, *3*, 3125–3128.
[62] M. Fujitsuka, D. W. Cho, T. Iwamoto, S. Yamago, T. Majima, *Phys. Chem. Chem. Phys.* **2012**, *14*, 14585–14588.
[63] Y. Segawa, A. Fukazawa, S. Matsuura, H. Omachi, S. Yamaguchi, S. Irle, K. Itami, *Org. Biomol. Chem.* **2012**, *10*, 5979–5984.
[64] M. R. Talipov, R. Jasti, R. Rathore, *J. Am. Chem. Soc.* **2015**, *137*, 14999–15006.
[65] H. W. Kroto, J. R. Heath, S. C. O'Brien, R. F. Curl, R. E. Smalley, *Nature* **1985**, *318*, 162–163.
[66] A. Sygula, F. R. Fronczek, R. Sygula, P. W. Rabideau, M. M. Olmstead, *J. Am. Chem. Soc.* **2007**, *129*, 3842–3843.
[67] E. M. Pérez, N. Martín, *Pure Appl. Chem.* **2010**, *82*, 523–533.
[68] M. Takeda, S. Hiroto, H. Yokoi, S. Lee, D. Kim, H. Shinokubo, *J. Am. Chem. Soc.* **2018**, *140*, 6336–6342.
[69] Y. Yang, M. Juríček, *ChemPlusChem* **2022**, *87*, e202100468.
[70] N. Grabicki, S. Fisher, O. Dumele, *Angew. Chem. Int. Ed.* **2023**, *62*, e202217917.
[71] Z. Sun, K. Ikemoto, M. F. Toshiya, T. Koretsune, R. Arita, S. Sato, H. Isobe, *Science* **2019**, *363*, 151–155.
[72] C. García-Simón, M. Costas, X. Ribas, *Chem. Soc. Rev.* **2016**, *45*, 40–62.
[73] W. Brenner, T. K. Ronson, J. R. Nitschke, *J. Am. Chem. Soc.* **2017**, *139*, 75–78.
[74] D. R. Evans, N. L. P. Fackler, Z. Xie, C. E. F. Rickard, P. D. W. Boyd, C. A. Reed, *J. Am. Chem. Soc.* **1999**, *121*, 8466–8474.
[75] P. D. W. Boyd, M. C. Hodgson, C. E. F. Rickard, A. G. Oliver, L. Chaker, P. J. Brothers, R. D. Bolskar, F. S. Tham, C. A. Reed, *J. Am. Chem. Soc.* **1999**, *121*, 10487–10495.
[76] M. M. Olmstead, D. A. Costa, K. Maitra, B. C. Noll, S. L. Phillips, P. M. Van Calcar, A. L. Balch, *J. Am. Chem. Soc.* **1999**, *121*, 7090–7097.
[77] D. Sun, F. S. Tham, C. A. Reed, L. Chaker, M. Burgess, P. D. W. Boyd, *J. Am. Chem. Soc.* **2000**, *122*, 10704–10705.
[78] T. Ishii, N. Aizawa, R. Kanehama, M. Yamashita, K.-i. Sugiura, H. Miyasaka, *Coordin. Chem. Rev.* **2002**, *226*, 113–124.
[79] C. Zhang, Q. Wang, H. Long, W. Zhang, *J. Am. Chem. Soc.* **2011**, *133*, 20995–21001.
[80] V. Leonhardt, S. Fimmel, A.-M. Krause, F. Beuerle, *Chem. Sci.* **2020**, *11*, 8409–8415.
[81] Y. Ni, F. Gordillo-Gámez, M. Peña Alvarez, Z. Nan, Z. Li, S. Wu, Y. Han, J. Casado, J. Wu, *J. Am. Chem. Soc.* **2020**, *142*, 12730–12742.
[82] Y.-Y. Xu, H.-R. Tian, S.-H. Li, Z.-C. Chen, Y.-R. Yao, S.-S. Wang, X. Zhang, Z.-Z. Zhu, S.-L. Deng, Q. Zhang, S. Yang, S.-Y. Xie, R.-B. Huang, L.-S. Zheng, *Nat. Commun.* **2019**, *10*, 485.
[83] J. Wang, Y.-Y. Ju, K.-H. Low, Y.-Z. Tan, J. Liu, *Angew. Chem. Int. Ed.* **2021**, *60*, 11814–11818.
[84] A. M. González-Delgado, J. J. Giner-Casares, G. Brezesinski, J.-B. Regnouf-de-Vains, L. Camacho, *Langmuir* **2012**, *28*, 12114–12121.
[85] J. Yang, L.-L. Mao, H. Xiao, G. Zhang, S. Zhang, L. Kang, Z. Lin, C.-H. Tung, L.-Z. Wu, H. Cong, *Angew. Chem. Int. Ed.* **2024**, *63*, e202403062.
[86] F. Zhang, X.-S. Du, K.-Z. Song, Y. Han, H.-Y. Lu, C.-F. Chen, *Chem. Commun.* **2024**, *60*, 4962–4965.
[87] J. Pfeuffer-Rooschüz, S. Heim, A. Prescimone, K. Tiefenbacher, *Angew. Chem. Int. Ed.* **2022**, *61*, e202209885.
[88] H. K. Chae, D. Y. Siberio-Pérez, J. Kim, Y. Go, M. Eddaoudi, A. J. Matzger, M. O'Keeffe, O. M. Yaghi, *Nature* **2004**, *427*, 523–527.
[89] S. Goswami, D. Ray, K.-i. Otake, C.-W. Kung, S. J. Garibay, T. Islamoglu, A. Atilgan, Y. Cui, C. J. Cramer, O. K. Farha, J. T. Hupp, *Chem. Sci.* **2018**, *9*, 4477–4482.
[90] T. Kawase, H. Kurata, *Chem. Rev.* **2006**, *106*, 5250–5273.
[91] T. Matsuno, S. Sato, H. Isobe, in *Comprehensive Supramolecular Chemistry II* (Ed.: J. L. Atwood), Elsevier, Oxford **2017**, pp. 311–328.
[92] C. Fuertes-Espinosa, M. Pujals, X. Ribas, *Chem* **2020**, *6*, 3219–3262.
[93] J. W. Steed, P. C. Junk, J. L. Atwood, M. J. Barnes, C. L. Raston, R. S. Burkhalter, *J. Am. Chem. Soc.* **1994**, *116*, 10346–10347.
[94] M. J. Hardie, P. D. Godfrey, C. L. Raston, *Chem. - Eur. J.* **1999**, *5*, 1828–1833.
[95] T. Suzuki, K. Nakashima, S. Shinkai, *Chem. Lett.* **1994**, *23*, 699–702.
[96] N. S. Isaacs, P. J. Nichols, C. L. Raston, C. A. Sandova, D. J. Young, *Chem. Commun.* **1997**, 1839–1840.
[97] T. Ogoshi, N. Ueshima, F. Sakakibara, T.-a. Yamagishi, T. Haino, *Org. Lett.* **2014**, *16*, 2896–2899.
[98] J. L. Atwood, L. J. Barbour, C. L. Raston, *Cryst. Growth & Des.* **2002**, *2*, 3–6.
[99] M. Makha, C. L. Raston, A. N. Sobolev, P. Turner, *Cryst. Growth & Des.* **2006**, *6*, 224–228.
[100] S. Bähring, K. R. Larsen, M. Supur, K. A. Nielsen, T. Poulsen, K. Ohkubo, C. W. Marlatt, E. Miyazaki, K. Takimiya, A. H.

Flood, S. Fukuzumi, J. O. Jeppesen, *Chem. Commun.* **2017**, *53*, 9898–9901.
[101] B. Chen, J. J. Holstein, S. Horiuchi, W. G. Hiller, G. H. Clever, *J. Am. Chem. Soc.* **2019**, *141*, 8907–8913.
[102] R. S. Ruoff, D. S. Tse, R. Malhotra, D. C. Lorents, *J. Phys. Chem.* **1993**, *97*, 3379–3383.
[103] P. Thordarson, *Chem. Soc. Rev.* **2011**, *40*, 1305–1323.
[104] S. Lee, C.-H. Chen, A. H. Flood, *Nat. Chem.* **2013**, *5*, 704–710.
[105] Y. Li, M. Pink, J. A. Karty, A. H. Flood, *J. Am. Chem. Soc.* **2008**, *130*, 17293–17295.
[106] E. Kleinpeter, S. Klod, A. Koch, *J. Org. Chem.* **2008**, *73*, 1498–1507.
[107] Y. Yamamoto, E. Tsurumaki, K. Wakamatsu, S. Toyota, *Angew. Chem. Int. Ed.* **2018**, *57*, 8199–8202.
[108] K. F. Morris, C. S. Johnson, Jr., *J. Am. Chem. Soc.* **1992**, *114*, 3139–3141.
[109] V. N. Bezmel'nitsyn, A. V. Eletskii, M. V. Okun, *Phys. Usp.* **1998**, *41*, 1091–1114.
[110] H. Iloukhani, B. Samiey, *J. Chem. Eng. Data* **2005**, *50*, 1911–1916.
[111] K. S. Cameron, L. Fielding, *Magn. Reson. Chem.* **2002**, *40*, S106–S109.
[112] A. I. Oliva, K. Gómez, G. González, P. Ballester, *New J. Chem.* **2008**, *32*, 2159–2163.
[113] E. Ruzicka, P. Pellechia, B. C. Benicewicz, *Anal. Chem.* **2023**, *95*, 7849–7854.
[114] supramolecular, http://supramolecular.org/ (accessed: April 2024).
[115] K. Tashiro, T. Aida, *Chem. Soc. Rev.* **2007**, *36*, 189–197.
[116] E. M. Pérez, N. Martín, *Chem. Soc. Rev.* **2008**, *37*, 1512–1519.
[117] X. Chang, Y. Xu, M. Delius, *Chem. Soc. Rev.* **2024**, *53*, 47–83.
[118] M. Nishio, *CrystEngComm* **2004**, *6*, 130–158.
[119] C. Janiak, *J. Chem. Soc. Dalton* **2000**, 3885–3896.
[120] T. Lu, Q. Chen, *J. Comput. Chem.* **2022**, *43*, 539–555.
[121] D. H. Williams, M. S. Westwell, *Chem. Soc. Rev.* **1998**, *27*, 57–64.
[122] K. N. Houk, A. G. Leach, S. P. Kim, X. Zhang, *Angew. Chem. Int. Ed.* **2003**, *42*, 4872–4897.
[123] A. Carboni, E. Emke, J. R. Parsons, K. Kalbitz, P. de Voogt, *Anal. Chim. Acta* **2014**, *807*, 159–165.
[124] H. Yi, G. Zeng, C. Lai, D. Huang, L. Tang, J. Gong, M. Chen, P. Xu, H. Wang, M. Cheng, C. Zhang, W. Xiong, *Chem. Eng. J.* **2017**, *330*, 134–145.
[125] Data obtained from Sigma-Aldrich Product Specification sheet, https://www.sigmaaldrich.com/specification-sheets/297/045/572497-BULK_____ALDRICH__.pdf (Data accessed Sep, 2024).
[126] M. Yamada, T. Akasaka, S. Nagase, *Angew. Chem. Int. Ed.* **2018**, *57*, 13394–13405.
[127] C.-R. Wang, Z.-Q. Shi, L.-J. Wan, X. Lu, L. Dunsch, C.-Y. Shu, Y.-L. Tang, H. Shinohara, *J. Am. Chem. Soc.* **2006**, *128*, 6605–6610.
[128] X. Han, S.-J. Zhou, Y.-Z. Tan, X. Wu, F. Gao, Z.-J. Liao, R.-B. Huang, Y.-Q. Feng, X. Lu, S.-Y. Xie, L.-S. Zheng, *Angew. Chem. Int. Ed.* **2008**, *47*, 5340–5343.
[129] G.-J. Shan, Y.-Z. Tan, T. Zhou, X.-M. Zou, B.-W. Li, C. Xue, C.-X. Chu, S.-Y. Xie, R.-B. Huang, L.-S. Zhen, *Chem. Asian J.* **2012**, *7*, 2036–2039.
[130] H.-R. Tian, M.-M. Chen, K. Wang, Z.-C. Chen, C.-Y. Fu, Q. Zhang, S.-H. Li, S.-L. Deng, Y.-R. Yao, S.-Y. Xie, R.-B. Huang, L.-S. Zheng, *J. Am. Chem. Soc.* **2019**, *141*, 6651–6657.
[131] C.-l. Gao, L. Abella, Y.-Z. Tan, X.-Z. Wu, A. Rodríguez-Fortea, J. M. Poblet, S.-Y. Xie, R.-B. Huang, L.-S. Zheng, *Inorg. Chem.* **2016**, *55*, 6861–6865.
[132] K. S. Simeonov, K. Y. Amsharov, M. Jansen, *Angew. Chem. Int. Ed.* **2007**, *46*, 8419–8421.
[133] I. N. Ioffe, A. A. Goryunkov, N. B. Tamm, L. N. Sidorov, E. Kemnitz, S. I. Troyanov, *Angew. Chem. Int. Ed.* **2009**, *48*, 5904–5907.
[134] K. S. Simeonov, K. Y. Amsharov, E. Krokos, M. Jansen, *Angew. Chem. Int. Ed.* **2008**, *47*, 6283–6285.
[135] C.-R. Wang, T. Sugai, T. Kai, T. Tomiyama, H. Shinohara, *Chem. Commun.* **2000**, 557–558.
[136] Y. Miyake, T. Minami, K. Kikuchi, M. Kainosho, Y. Achiba, *Molecular Crystals and Liquid Crystals Science and Technology. Section A. Molecular Crystals and Liquid Crystals* **2000**, *340*, 553–558.
[137] Z. Wang, H. Yang, A. Jiang, Z. Liu, M. M. Olmstead, A. L. Balch, *Chem. Commun.* **2010**, *46*, 5262–5264.
[138] A. R. Khamatgalimov, V. I. Kovalenko, *Int. J. Quantum Chem.* **2011**, *111*, 2966–2971.
[139] H. Yang, C. M. Beavers, Z. Wang, A. Jiang, Z. Liu, H. Jin, B. Q. Mercado, M. M. Olmstead, A. L. Balch, *Angew. Chem. Int. Ed.* **2010**, *49*, 886–890.
[140] R. M. Koenig, H.-R. Tian, T. L. Seeler, K. R. Tepper, H. M. Franklin, Z.-C. Chen, S.-Y. Xie, S. Stevenson, *J. Am. Chem. Soc.* **2020**, *142*, 15614–15623.
[141] X. Liu, E. Bourret, C. A. Noble, K. Cover, R. M. Koenig, R. Huang, H. M. Franklin, X. Feng, R. J. Bodnar, F. Zhang, C. Tao, D. M. Sublett, Jr., H. C. Dorn, S. Stevenson, *J. Am. Chem. Soc.* **2022**, *144*, 16287–16291.
[142] H. Yang, H. Jin, Y. Che, B. Hong, Z. Liu, J. A. Gharamaleki, M. M. Olmstead, A. L. Balch, *Chem. - Eur. J.* **2012**, *18*, 2792–2796.
[143] C. S. Johnson, *Prog. Nuc. Mag. Res. Spec.* **1999**, *34*, 203–256.
[144] T. D. W. Claridge, in *Tetrahedron Organic Chemistry Series*, Vol. *27* (Ed.: T. D. W. Claridge), Elsevier, **2009**, pp. 303–334.
[145] A. Spek, *J. Appl. Cryst.* **2003**, *36*, 7–13.
[146] A. Spek, *Acta Cryst. D* **2009**, *65*, 148–155.
[147] G. M. Sheldrick, *Acta Cryst. A* **2015**, *71*, 3–8.
[148] G. M. Sheldrick, *Acta Cryst. C* **2015**, *71*, 3–8.
[149] O. V. Dolomanov, L. J. Bourhis, R. J. Gildea, J. A. K. Howard, H. Puschmann, *J. Appl. Cryst.* **2009**, *42*, 339–341.
[150] M. J. Frisch, G. W. Trucks, H. B. Schlegel, G. E. Scuseria, M. A. Robb, J. R. Cheeseman, G. Scalmani, V. Barone, G. A. Petersson, H. Nakatsuji, X. Li, M. Caricato, A. V. Marenich, J. Bloino, B. G. Janesko, R. Gomperts, B. Mennucci, H. P. Hratchian, J. V. Ortiz, A. F. Izmaylov, J. L. Sonnenberg, Williams, F. Ding, F. Lipparini, F. Egidi, J. Goings, B. Peng, A. Petrone, T. Henderson, D. Ranasinghe, et al., Wallingford, CT, **2016**, https://gaussian.com/citation/
[151] A. D. Becke, *Phys. Rev. A Gen. Phys.* **1988**, *38*, 3098–3100.
[152] S. Grimme, S. Ehrlich, L. Goerigk, *J. Comput. Chem.* **2011**, *32*, 1456–1465.
[153] E. Cancès, B. Mennucci, J. Tomasi, *J. Chem. Phys.* **1997**, *107*, 3032–3041.
[154] T. Stadelmann, C. Balmer, S. Riniker, M.-O. Ebert, *Phys. Chem. Chem. Phys.* **2022**, *24*, 23551–23560.
[155] K. Wolinski, J. F. Hinton, P. Pulay, *J. Am. Chem. Soc.* **1990**, *112*, 8251–8260.
[156] N. M. O'Boyle, A. L. Tenderholt, K. M. Langner, *J. Comput. Chem.* **2008**, *29*, 839–845.
[157] W. Humphrey, A. Dalke, K. Schulten, *J. Mol. Graph.* **1996**, *14*, 33–38.
[158] T. Lu, F. Chen, *J. Comput. Chem.* **2012**, *33*, 580–592.
[159] I. Elidrisi, S. Negin, P. V. Bhatt, T. Govender, H. G. Kruger, G. W. Gokel, G. E. M. Maguire, *Org. Biomol. Chem.* **2011**, *9*, 4498–4506.

Manuscript received: March 03, 2025
Revised manuscript received: April 15, 2025
Accepted manuscript online: April 16, 2025
Version of record online: May 02, 2025